ECOSYSTEMS

Terrestrial Nitrogen Inputs Affect the Export of Unprocessed Atmospheric Nitrate to Surface Waters: Insights from Triple Oxygen Isotopes of Nitrate

Joel T. Bostic,[1]* David M. Nelson,[1] Robert D. Sabo,[2] and Keith N. Eshleman[1]

[1]University of Maryland Center for Environmental Science, Appalachian Lab, Frostburg, Maryland 21532, USA; [2]U.S. Environmental Protection Agency, Office of Research and Development, Center for Public Health and Environmental Assessment, U.S. EPA, Washington, District of Columbia, USA

ABSTRACT

Atmospheric nitrate ($NO_3^-{}_{Atm}$) deposition has increased dramatically during the past $\sim$ 150 years and contributes to ecosystem eutrophication. $NO_3^-{}_{Atm}$ deposition is widespread, but the role of different landscapes in modulating watershed-scale processing and export of $NO_3^-{}_{Atm}$ remains unclear. We measured triple oxygen isotopes (a tracer of $NO_3^-{}_{Atm}$) of NO_3^- for 832 stream samples collected during baseflow and stormflow from 14 watersheds of varied land use throughout two years in the Chesapeake Bay watershed, and we used these data to assess the influence of land use on $NO_3^-{}_{Atm}$ dynamics. Watersheds with more agricultural ($>$ 35%) and developed ($>$ 70%) land exported more $NO_3^-{}_{Atm}$ than predominantly forested ($>$ 75%) watersheds. Agricultural lands likely facilitate greater $NO_3^-{}_{Atm}$ export because of elevated rates of terrestrial N addition relative to rates of NO_3^- consumption. In contrast, developed lands likely have limited biotic processing of $NO_3^-{}_{Atm}$ because of greater hydrologic connectivity of overland flow pathways to channels. Our results, along with data from prior studies, can be interpreted by extending the conceptual model of kinetic N saturation to $NO_3^-{}_{Atm}$ streamwater export across varied land use watersheds. In this framework, elevated rates of terrestrial N inputs overwhelm NO_3^- sinks, allowing proportionally more $NO_3^-{}_{Atm}$ to leak from watersheds. Changes in watershed-scale N inputs that increase stream NO_3^- concentrations additively affect $NO_3^-{}_{Atm}$, with agricultural watersheds, and their associated large terrestrial N inputs, increasing $NO_3^-{}_{Atm}$ export.

Key words: water quality; hydrology; forest; atmospheric nitrate; land use; oxygen isotopes.

Author's Contribution: DN, RS, and KE designed the study. JB, DN, and KE performed field research. JB measured isotopes, analyzed data, and wrote the first draft. All authors contributed to manuscript revisions
*Corresponding author; e-mail: jbostic@umces.edu

HIGHLIGHTS

- Terrestrial N inputs and hydrology control patterns of atmospheric nitrate export
- Forested lands exported less atmospheric nitrate than more agricultural and developed lands
- The concept of kinetic N saturation can be applied to interpret atmospheric nitrate patterns across heterogenous watersheds

INTRODUCTION

Deposition of atmospheric nitrate ($NO_3^-{}_{Atm}$) has increased dramatically worldwide during about the past 150 years (Galloway and others 2004). Despite declines in recent decades in some regions (Tørseth and others 2012; Li and others 2016), deposition remains elevated and contributes to the eutrophication and acidification of terrestrial and aquatic ecosystems globally (Galloway and others 2003; Kemp and others 2005; Clark and Tilman 2008). The specific impacts of $NO_3^-{}_{Atm}$ partially depend on whether it is processed (incorporated into the terrestrial nitrogen cycle) or exported unprocessed to surface waters. Terrestrial processing of $NO_3^-{}_{Atm}$ can provide longer-term storage (that is, assimilation) or removal (that is, denitrification), whereas stream export can have more immediate impacts, such as exacerbating nutrient pollution of downstream waters (Howarth and others 2000). Understanding the factors controlling the relative amounts of $NO_3^-{}_{Atm}$ that are processed versus exported to streams is needed to evaluate potential impacts on affected ecosystems.

Landscape properties represent a potentially dominant factor regulating the proportion of (unprocessed) $NO_3^-{}_{Atm}$ deposition that is exported in streamwater. $NO_3^-{}_{Atm}$ occurs across broad spatial extents (Driscoll and others 2001) and thus impacts diverse landscapes. Different land uses (for example, forest, agriculture, developed) are commonly associated with generalizable patterns of streamwater NO_3^- export (Jordan and others 1997; Groffman and others 2004; Kaushal and others 2008) that can partially be attributed to variable amounts and sources of nitrogen (N) inputs (Lovett and Goodale 2011), differing rates of key N cycling processes and/or alterations of hydrologic flowpaths (Sudduth and others 2013)—all of which could influence processing of $NO_3^-{}_{Atm}$. For example, the conceptual kinetic N saturation model suggests that ecosystem N losses, including streamwater export, occur when rates of inputs (for example, from deposition, fertilizer) exceed sinks at various temporal scales (for example, vegetative uptake, immobilization; Lovett and Goodale 2011). This model was developed and has been applied to understand N deposition effects on streamwater NO_3^- export from predominantly forested watershed (Eshleman and others 2013), but it may be applicable to $NO_3^-{}_{Atm}$ processing and export from mixed land use watersheds with elevated N input rates (Eshleman and Sabo 2016). However, prior research into watershed cycling of $NO_3^-{}_{Atm}$ has focused primarily on predominantly forested or alpine watersheds (for example, Tsunogai and others 2010; Fang and others 2015; Osaka and others 2016; Bourgeois and others 2018a; Bourgeois and others 2018b; Sebestyen and others 2019) where deposition represents the primary input of N and streamwater NO_3 export is generally low. Thus, the relative importance of potential controls on $NO_3^-{}_{Atm}$ dynamics associated with variable land uses and elevated, non-deposition N inputs is unclear (Burns and others 2009; Tsunogai and others 2016). Assessing the potential effects of land use on the fate of $NO_3^-{}_{Atm}$ requires accurate accounting of streamwater $NO_3^-{}_{Atm}$ export across watersheds with varied N sources, magnitudes of NO_3^- export, and hydrologic conditions, but this remains a major challenge.

Many prior studies have used $\delta^{18}O$ values of NO_3^- in streamwater to distinguish atmospheric and terrestrial fractions (Kendall and others 1995; Burns and Kendall 2002; Burns and others 2009; Kaushal and others 2011). This approach takes advantage of $NO_3^-{}_{Atm}$ having elevated $\delta^{18}O$ values (~ 60–$90‰$) relative to NO_3^- of terrestrial origin ($\delta^{18}O \cong -15$—$+15‰$; Kendall and others 2007; Michalski and others 2012). However, interpretation of $\delta^{18}O$ as a tracer of $NO_3^-{}_{Atm}$ is complicated by many factors. For example, NO_3^- consumption (plant or microbial uptake, denitrification) can elevate the $\delta^{18}O$ values of residual NO_3^- resulting in potentially overlapping ranges of $\delta^{18}O$ values of terrestrial and atmospheric NO_3^- (Böttcher and others 1990; Kendall and others 2007). Additionally, dilution of the $\delta^{18}O$ $NO_3^-{}_{Atm}$ signal is likely to be greatest in watersheds with high loads of streamwater NO_3^- export relative to atmospheric inputs (that is, agricultural watersheds), which, when combined with the large range of terrestrial $\delta^{18}O$ values, can obscure the $NO_3^-{}_{Atm}$ signal. These complications are mitigated by an increasingly used tracer of $NO_3^-{}_{Atm}$, triple oxygen isotopes of NO_3^-:

$$\Delta^{17}O = \left(\frac{1 + \delta^{17}O}{(1 + \delta^{18}O)^{\beta}} - 1 \right) \times 1000 \qquad (1)$$

where $\delta = (R_{sample}/R_{reference}) - 1$, R = ratio of heavy to light isotope, and $\beta \cong 0.52$ (Michalski and others 2003). The $\Delta^{17}O$ value of terrestrial NO_3^- is $\cong 0\permil$ (Kendall and others 2007), and relative to $\delta^{18}O$, the $\Delta^{17}O$ values of $NO_3^-_{Atm}$ (~ 20–$30\permil$ in the mid-latitudes; Tsunogai and others 2010; Rose and others 2015; Tsunogai and others 2016; Bourgeois and others 2018b; Nelson and others 2018) in residual NO_3^- change minimally during biological processing (Young and others 2002; Michalski and others 2004; Kendall and others 2007). Furthermore, dilution of $\Delta^{17}O$ values of $NO_3^-_{Atm}$ can occur, but the small range of $\Delta^{17}O$ values for terrestrial NO_3^- ($\sim 0\permil$) allows for more accurate quantification of $NO_3^-_{Atm}$, even in watersheds with high rates of streamwater NO_3^- export relative to deposition.

Measurements of nitrate $\Delta^{17}O$ only allow for quantification of unprocessed $NO_3^-_{Atm}$ because they ''trace'' NO_3^- produced in the atmosphere. Terrestrial N cycling (immobilization, assimilation, mineralization, and nitrification) only retains the N atom of NO_3^-. Thus, there is a distinction between processing and retention (that is, proportion of NO_3^- inputs that are exported in streamwater on an annual basis) of deposited $NO_3^-_{Atm}$. For example, a $NO_3^-_{Atm}$ molecule could theoretically be deposited, undergo terrestrial N cycling (that is, become immobilized, mineralized, then nitrified), and be exported as NO_3^- in streamwater a short time later (that is, days or weeks post-deposition), and would be considered processed (that is, the molecule would have a $\Delta^{17}O \cong 0$) but not retained. Thus, the fraction of $NO_3^-_{Atm}$ deposition that is processed represents the upper limit of watershed retention (that is, $NO_3^-_{Atm}$ processing $\geq$ retention).

Estimates of mean annual streamwater nitrate-$\Delta^{17}O$ and $NO_3^-_{Atm}$ loads, which are not equivalent, provide a useful framework for assessing the relative rates of watershed-scale NO_3^- consumption (denitrification, immobilization, or assimilation) and addition (nitrification, fertilization; Figure 1). The relative rates of these processes affect both $NO_3^-_{Atm}$ and total NO_3^- ($NO_3^-_{Total}$) cycling and streamwater export across diverse land uses. The difference in the mass of $NO_3^-_{Atm}$ deposited and exported in streams is caused by NO_3^- consumption processes along hydrologic flowpaths, which do not alter the $\Delta^{17}O$ value of the residual NO_3^- (Böttcher and others 1990; Michalski and others 2004; Kendall and others 2007). Reduction in the $\Delta^{17}O$ value of deposited NO_3^- is caused by the addition of new microbially or synthetically sourced nitrate or dilution by existing terrestrial NO_3^- (for example, synthetic fertilizer, nitrification) with $\Delta^{17}O \cong 0\permil$ (Kendall and others 2007) encountered along hydrologic flowpaths. This framework for assessing relative rates of watershed-scale NO_3^- consumption and addition is primarily possible because of the unique triple oxygen isotopic tracer of $NO_3^-_{Atm}$, but also due to the widespread deposition of $NO_3^-_{Atm}$ across watersheds (Driscoll and others 2001) and the relative mobility of NO_3^- (Chapin and others 2011). By quantifying the processing and export of $NO_3^-_{Atm}$ across watersheds with varied land use, we use this framework to assess watershed-scale N cycling dynamics.

Here we ask the following questions: How do terrestrial N inputs and land use influence the cycling and surface water export of $NO_3^-_{Atm}$ at the watershed scale? More specifically, what is the relationship between terrestrial N inputs, the proportion of major land use categories (forest, agriculture, and developed) in watersheds and $NO_3^-_{Atm}$ concentrations, yields, and processing efficiency (that is, fraction of $NO_3^-_{Atm}$ deposition that is processed prior to surface water export)? To address these questions, we measured $\Delta^{17}O$ values of NO_3^- on 832 stream samples collected during both baseflow and stormflow conditions from 14 watersheds of varied land use in the Chesapeake Bay watershed in eastern North America during a two-year period. We hypothesize that predominantly forested watersheds with lower terrestrial N inputs will have lower $NO_3^-_{Atm}$ concentrations and yields, and higher processing efficiency, than watersheds that are predominantly agricultural and/or developed with higher rates of terrestrial N inputs. If our results show that increased $NO_3^-_{Atm}$ concentrations are positively related to terrestrial N inputs, it would provide support for extending the kinetic N saturation conceptual model to $NO_3^-_{Atm}$ streamwater export across varied land use watersheds.

MATERIALS AND METHODS

Study Sites and Field Methods

To assess land use effects on $NO_3^-_{Atm}$ dynamics across a range of hydroclimatological conditions, streamwater samples were collected from 14 watersheds varying in size (160–127,900 ha), dominant land use (96% forest to 70% developed), and mean annual temperature and precipitation
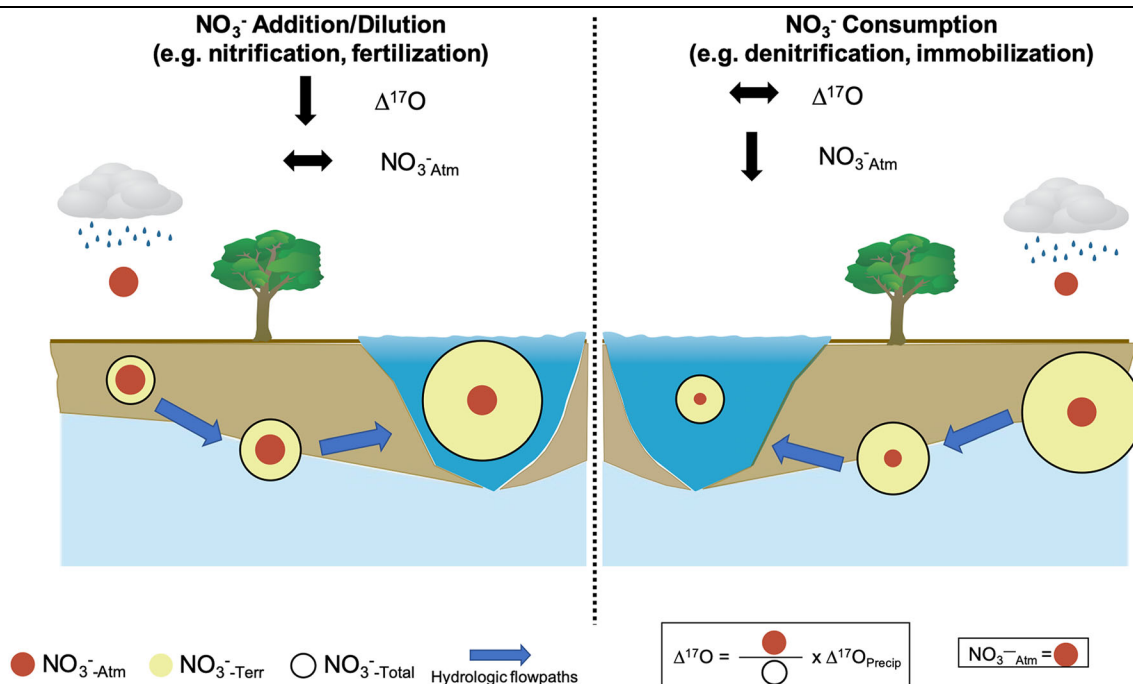
Figure 1. Framework for interpreting variation in $\Delta^{17}O$- NO_3^- and $NO_3^-{}_{Atm}$ concentrations. These indicators provide different, yet complementary information about watershed-scale N cycling processes. $\Delta^{17}O$ of nitrate is equal to the fraction of $NO_3^-{}_{Atm}$ (red circles) relative to $NO_3^-{}_{Total}$ (black circles, sum of $NO_3^-{}_{Terr}$ and $NO_3^-{}_{Atm}$) multiplied by the $\Delta^{17}O$ of deposition. Left panel) Addition of $NO_3^-{}_{Terr}$ or dilution of $NO_3^-{}_{Atm}$ by $NO_3^-{}_{Terr}$ decreases the $\Delta^{17}O$ of a "reservoir" of NO_3^- by increasing $NO_3^-{}_{Total}$ along hydrologic flowpaths prior to export in streamwater, which is illustrated by the increasing area of the black outlined circle relative to $NO_3^-{}_{Atm}$ (red square). Addition of $NO_3^-{}_{Terr}$ does not change the concentration of $NO_3^-{}_{Atm}$ (area of the red circle). Right panel) NO_3^- consumption (for example, denitrification, assimilation, immobilization) processes reduce the concentration of $NO_3^-{}_{Atm}$ from deposition, along hydrologic flowpaths, before eventual export in streamwater, but does not change the $\Delta^{17}O$ value of residual nitrate (indicated by the constant area of the black outlined circle relative to $NO_3^-{}_{Atm}$, the red circle). NO_3^- consumption is a mass-dependent fractionation process and therefore does not alter the $\Delta^{17}O$ (result of mass-independent fractionation processes) of the NO_3^- reservoir.

(Table 1). Streamwater grab samples (120–1000 mL) were collected both regularly (2 samples per month) and irregularly during storm events ($\sim$ 6–10 samples per year; n = 57–65 total samples per watershed) from the outlets of 14 gaged watersheds within the Chesapeake Bay basin from October 2015–September 2017 (that is, water years 2016 and 2017; Figures S1 and S2). Samples were collected in pre-cleaned polypropylene bottles and kept on ice for 2–4 h before being refrigerated until they were then processed in the laboratory within 24–48 h. Sampling across a range of hydrological conditions (Figure S2) was done to more fully capture streamwater $NO_3^-{}_{Atm}$ variation and to improve accuracy of estimated $NO_3^-{}_{Atm}$ loads. Estimated loads of many other streamwater constituents (total nitrogen, total NO_3^-, total phosphorus, and so on) are more accurate when samples are collected over a range of hydrological conditions (Sprague 2001). Daily stream discharge data were obtained from U.S. Geological Survey

records for ten of the study watersheds. Stream discharge in the other four watersheds (Table 1) was measured by the authors using comparable stream gaging practices. These practices involve development of a rating curve (log–log regression of discharge vs. stage) for each station and computation of mean daily discharge based on hourly stage data from a digital water level recorder. Weekly precipitation samples during water year (WY) 2017 were obtained from three National Atmospheric Deposition Program (NADP) sites (PA00, MD99, and MD08) bounding the study watersheds (Figure S1). Precipitation NO_3^- concentration and isotope data are summarized in the Supporting Information (SI). Land use percentages were calculated from the 2016 National Land Cover Database; agricultural land represents the sum of both cultivated crop and pasture/hay land classes (Homer and others 2020). Mean watershed slope (m/m) was obtained using the U.S. Geological Survey StreamStats program (USGS 2016).

Table 1. Watershed Attributes

Watershed	Area (ha)	USGS Gage	Land use (%)			Terrestrial N Inputs (kg N ha^{-1} y^{-1})	MAT (°C)	MAP (cm)	NO$_3^-$ monitoring record (yrs)	Slope (m/m)
			Forest	Agriculture	Developed					
Antietam Upstream (ANT)	24,200	01619000	41.3	41.8	15.9	64.16	12.2	107	13	0.10
Antietam Downstream (ANT2)	72,800	01619500	29.2	51.9	17.7	64.94	12.6	101	33	0.08
Big Run (BIGR)	160	n/a	89.4	0	10.1	2.16	9.7	123	27	0.22
Black Lick (BLAC)	560	n/a	85.7	12.6	0.8	13.35	9.9	112	21	0.22
Catoctin Creek (CAC)	17,300	01637500	51.7	37.7	10	40.73	12.6	105	33	0.12
Conococheague Creek (CON)	127,900	01614500	38.4	47.0	13.3	68.75	12.3	103.2	33	0.10
Deep Run (DPRN)	1,620	n/a	96.2	1.0	2.7	1.25	11.9	101	13	0.23
Georges Creek (GEO)	18,800	01599000	76.9	8.8	8.3	8.72	10.4	112.0	33	0.16
Gunpowder Falls (GUN)	41,400	01582500	45.4	41.3	10.9	45.53	13.1	111.3	33	0.10
Gwynns Falls (GWN)	8,400	01589300	23.4	5.0	70.1	11.04	13.7	112.1	15	0.06
Monocacy River (MON)	44,800	01639000	25.6	57.1	13.5	52.67	12.5	105.7	33	0.05
Terrapin Run (TERR)	570	n/a	87.5	2.1	10.5	3.67	11.9	108.9	11	0.17
Town Creek (TOW)	38,300	01609000	83.9	11.8	3.9	10.00	11.6	104.2	11	0.20
Wills Creek (WIL)	64,000	01601500	82.3	11.7	5.5	12.82	10.8	108.4	33	0.21

Land use data were compiled from the 2016 National Land Cover Database (Homer and others 2020). Land use percentages do not sum to 100% as all land use classes are not listed (for example, open water, wetlands), n/a not applicable; MAT Mean Annual Temperature, MAP Mean Annual Precipitation. Note that MAT and MAP are for WY 2016–2017.

Laboratory Methods

Stream samples were filtered (0.45 μm) and frozen within 48 h of collection. Stream NO_3^- and nitrite (NO_2^-) concentrations were measured using flow-injection colorimetric analysis (Lachat Quickchem 8000 FIA +). Weekly precipitation NO_3^- concentration data were provided by the NADP Central Analytical Laboratory (NADP 2021).

Triple oxygen isotopes (^{16}O, ^{17}O, and ^{18}O) of stream and precipitation NO_3^- were measured using a Thermo Delta V+ isotope ratio mass spectrometer (Bremen, Germany) via the denitrifier method (Sigman and others 2001; Casciotti and others 2002) with thermal decomposition (at 800° C) of N_2O to N_2 and O_2 at the Central Appalachians Stable Isotope Facility (Kaiser and others 2007). NO_2^- is denitrified using this method as well, but NO_2^- concentrations in stream and precipitation samples were low relative to NO_3^- (NO_2^-/ (NO_2^- + NO_3^-) mean = 0.01, range = 0.00–0.11). Measured oxygen isotope ratios were calibrated to international reference standards USGS 34 ($\delta^{17}O = -14.8‰$, $\delta^{18}O = -27.9‰$) and USGS 35 ($\delta^{17}O = 51.5‰$, $\delta^{18}O = 57.5‰$; Böhlke and others 2003) measured throughout sample analysis in equal concentrations to samples (ranging from 100–200 nmol depending on sample NO_3^- concentration). Analytical precision of $\Delta^{17}O$ values of NO_3^- was 0.5‰ (1σ) as determined by repeated measurements ($n \cong 200$) of international reference standard USGS 32 (mean measured $\Delta^{17}O \cong -0.2‰$) and laboratory reference standard ''Chile NO_3^-'' (Duda Energy 1sn 1 lb. Sodium Nitrate Fertilizer 99+ % Pure Chile Saltpeter from Amazon.com; mean measured $\Delta^{17}O \cong 19.7‰$) made during runs associated with these streamwater samples over 3+ years. Additionally, streamwater sample replicates were analyzed ($n = 60$) and had a pooled standard deviation of 0.5‰. Accuracy of $\Delta^{17}O$ was tracked using repeated measurements of IAEA-N3 ($n = 19$, μ = −0.1‰, 1 σ = 0.5‰) and closely agreed with published values of −0.2‰ (Michalski and others 2002; Böhlke and others 2003).

Quantification of Unprocessed Atmospheric NO_3^- in Streams and Uncertainty Estimation

Mean streamwater nitrate- $\Delta^{17}O$ ($\overline{\Delta^{17}O_{Stream}}$) for each watershed was calculated over the entire study period to provide an aggregate estimate of watershed response. Analytical uncertainty of individually measured $\Delta^{17}O$ samples was incorporated into $\overline{\Delta^{17}O_{Stream}}$ by sampling with replacement (that is, bootstrapping) from a probability density function that incorporated both normal and uniform distributions (additional details are provided in the SI). $\overline{\Delta^{17}O_{Stream}}$ was used to calculate the mean percentage of unprocessed $NO_3^-_{Atm}$ in stream samples using Eq. 2:

$$\%NO_3^-_{Atm} = \frac{\left(\overline{\Delta^{17}O_{Stream}} - \Delta^{17}O_{Terr}\right)}{\left(\Delta^{17}O_{Precip} - \Delta^{17}O_{Terr}\right)} \times 100 \quad (2)$$

where $\overline{\Delta^{17}O_{Precip}}$ = mean $\Delta^{17}O$ of wet NO_3^- deposition during WY2017, and $\Delta^{17}O_{Terr}$ = $\Delta^{17}O$ of terrestrially sourced NO_3^-. We assumed that the annual mean isotopic composition of NO_3^- in precipitation did not significantly differ between WY2016 and WY2017. Data from a three-year record in the mid-latitudes (inter-annual range = 1.5‰) suggest this assumption is reasonable (Tsunogai and others 2016). Uncertainty in % $NO_3^-_{Atm}$ from all three parameters in Eq. 2 and was estimated using bootstrapping methods. Values for each parameter in Eq. 2 were randomly sampled from distributions that accounted for analytical uncertainty ($\Delta^{17}O_{Stream}$), natural intra-annual variation ($\Delta^{17}O_{Precip}$), and potential variability in β values ($\Delta^{17}O_{Terr}$) during mass-dependent fractionation processes (for example, nitrification, denitrification) that could generate non-zero $\Delta^{17}O$ values not attributable to $NO_3^-_{Atm}$ (Young and others 2002; Kaiser and others 2007). This approach resulted in a distribution of % $NO_3^-_{Atm}$ that was then used to propagate uncertainty (that is, sample from this distribution with replacement) through additional calculations. The $\Delta^{17}O$ value of terrestrial NO_3^- is commonly assumed to be exactly 0‰ (Sabo and others 2016; Tsunogai and others 2016; Nakagawa and others 2018; but see Rose and others 2015), but previous studies reported negative values 3–4 times beyond the standard deviation of instrument uncertainty (Rose and others 2015; Yu and Elliott 2018) suggesting that β values are not necessarily stable during complex N cycling reactions and/or $\Delta^{17}O$ of terrestrial NO_3^- is not always equal to 0‰. Our approach attempts to account for some of these yet unquantified effects that may cause $\Delta^{17}O$ of terrestrial NO_3^- to deviate from 0‰ by allowing β to vary from 0.51–0.53. Additional details of uncertainty estimation and propagation are provided in the SI.

We acknowledge that natural, or ''organic'', NO_3^- fertilizers (for example, mined from desert deposits and classified as organic) can have

$\Delta^{17}O > 0‰$ (Michalski and others [2015]). No data on application of this NO_3^- fertilizer use exist for our watersheds, although it represents a minor percentage ($< 0.01\%$) of N fertilizer applied nationally since ~ 1970 (Böhlke and others [2009]). Mean annual flow-weighted concentrations and yields of $NO_3^-{}_{Atm}$ were quantified using Eq. [3]:

$$NO_{3Atm}^- = \%NO_{3Atm}^- \times NO_{3Total}^- \quad (3)$$

where $NO_3^-{}_{Total} =$ either annual flow-weighted concentrations (mg N L^{-1}) or yields (kg N ha^{-1}) of $NO_3^-{}_{Total}$.

Daily $NO_3^-{}_{Total}$ loads (L_{NO3}, kg d^{-1}) were computed using Weighted Regression on Time, Discharge, and Season-Kalman Filter (WRTDS-K; (Zhang and Hirsch [2019]). Models were calibrated using the entire period of record for $NO_3^-{}_{Total}$ (11–33 years). The use of the entire record ensured that model coefficients were representative of a greater range of hydroclimatological conditions than was realized in two water years. Estimated daily loads of $NO_3^-{}_{Total}$ were summed for WY2016–2017, normalized by watershed area and divided by the period of record (2 years) to compute annual average yields (kg N ha^{-1} y^{-1}). Flow-weighted annual mean concentrations were calculated by dividing annualized loads by annual discharge for WY2016–2017. $NO_3^-{}_{Total}$ uncertainty (annual concentrations and yields) was estimated using block bootstrapping methods and are detailed in the SI. $NO_3^-{}_{Atm}$ uncertainty (concentrations and yields) incorporated both $NO_3^-{}_{Total}$ and % $NO_3^-{}_{Atm}$ uncertainty through bootstrapping, or sampling with replacement from distributions of both $NO_3^-{}_{Total}$ and % $NO_3^-{}_{Atm}$.

NO_3^- Deposition

Grids of NO_3^- in wet deposition were generated using NO_3^- concentration data and point precipitation data from NADP and gridded precipitation data from the PRISM Climate Group for WY2016–2017 (PRISM Climate Group [2004]). Interpolated surfaces of monthly precipitation-weighted NO_3^- were generated using inverse distance weighting and then multiplied by PRISM precipitation data to produce water year NO_3^- deposition grids. Watershed-scale mean NO_3^- wet deposition was computed as the areal average of deposition within the watershed boundary.

Processing Efficiency of Atmospheric NO_3^-

Processing efficiency (PE), defined as the percentage of deposited NO_3^- that is incorporated into the terrestrial N cycle (that is, $\Delta^{17}O$ is reset to $\cong 0‰$) prior to stream export, which builds on a similar metric as Barnes and others ([2008]), was calculated as:

$$PE = \left(1 - \frac{NO_{3Atm}^- \left(\text{kg N ha}^{-1} \text{ yr}^{-1}\right)}{NO_{3Precip}^- \left(\text{kg N ha}^{-1} \text{ yr}^{-1}\right)}\right) \times 100 \quad (4)$$

NO_3^- in wet deposition was used for this calculation. It has previously been assumed that dry NO_3^- deposition is similar in magnitude to wet NO_3^- deposition (Lovett and Lindberg [1993]; Boyer and others [2002]; Grigal [2012]; Eshleman and Sabo [2016]), which implies that PE values are uniformly underestimated across all watersheds. Scenarios in which this assumption may be violated are presented in the SI. PE uncertainty was estimated from bootstrapped distributions of $NO_3^-{}_{Atm}$ yield.

Terrestrial N Inputs

Rates of terrestrial N inputs (in kg N ha^{-1} y^{-1}) to watersheds were obtained from the Chesapeake Bay Program Chesapeake Assessment and Scenario Tool (Chesapeake Bay Program [2020]). Estimates of terrestrial N inputs are made at the county scale and assigned to specific land uses (for example, developed, agriculture). These inputs were aggregated to the watershed scale by calculating the percentage of each land use in different counties for all study watersheds.

Statistical Analyses

Weighted least squares regression (dependent variables weighted by $1/\sigma$, where σ = standard deviation) of mean annual $\Delta^{17}O$ values, $NO_3^-{}_{Atm}$ concentrations, and PE to land use percentages and terrestrial N input rates was used to estimate slopes because of the non-uniform error in y-values (Bevington and Robinson [2003]). The coefficient of determination (r^2) was used to assess regression fit, and r^2 values are reported as the median of all bootstrapped replicates. Significance of linear regression slopes was determined via bootstrapping at $\alpha = 0.05$; reported p-values are the proportion of 10,000 slope estimates that are either greater than or less than zero (depending on the direction of the relationship). Welch's ANOVA was used, due to heterogeneity of variances, to compare means (that is, $\Delta^{17}O$, $NO_3^-{}_{Atm}$) between individual watersheds,
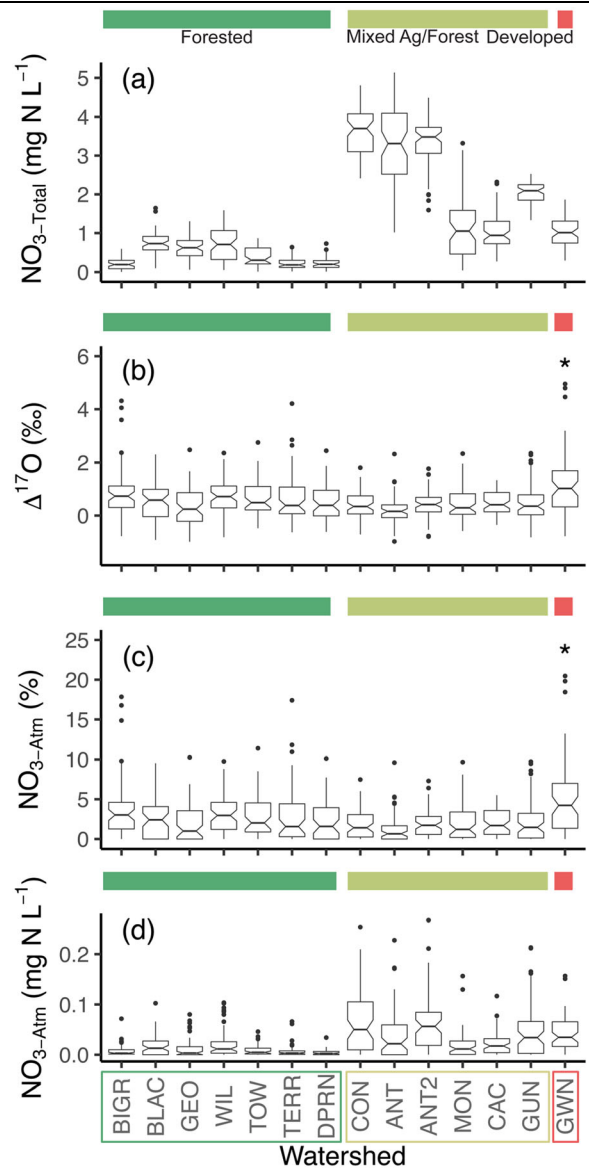
watersheds grouped by dominant land use and rates of terrestrial N inputs, and across flow conditions (McDonald 2009). All statistical analyses were performed in R (R Development Core Team 2019).

RESULTS

Mean annual precipitation NO_3^- concentrations ranged from 0.140–0.160 mg N L^{-1} and wet NO_3^- deposition ranged from 1.47–1.77 kg N ha^{-1} y^{-1} during WY 2016–2017 (Table S1). Annual areal mean precipitation depth ranged from 101–123 cm (Table S1). $\Delta^{17}O$ values of precipitation NO_3^- ranged from 16.4–29.3‰ with elevated values in the winter and lower values in the summer (Figure S3) and a depth-weighted annual mean (± standard error) of 25.2‰ ± 0.3‰.

In individual streamwater samples, $NO_3^-{}_{Total}$ concentrations ranged from 0.001–5.139 mg N L^{-1} and yields of $NO_3^-{}_{Total}$ ranged from 0.60–11.64 kg N ha^{-1} y^{-1} (Figure 2; Table S2). Values of $\Delta^{17}O$ in individual stream samples ranged from −1.0–5.0‰, corresponding to % $NO_3^-{}_{Atm}$ from 0–21% (Figure 2), and $\delta^{18}O$ ranged from −11.5–14.8‰ (Figure S4). $NO_3^-{}_{Atm}$ concentrations in individual samples, calculated using $NO_3^-{}_{Total}$ and $\Delta^{17}O$, ranged from 0–0.267 mg N L^{-1}. Averaged over the entire study period (WY2016–2017), $\overline{\Delta^{17}O}_{Stream}$ ranged from 0.2–1.3‰ across watersheds, representing 1–5% $NO_3^-{}_{Atm}$, and mean flow-weighted $NO_3^-{}_{Atm}$ concentrations ranged from 0.007–0.062 mg N L^{-1} (Table S2). Yields of $NO_3^-{}_{Atm}$ ranged from 0.03–0.30 kg N ha^{-1} yr^{-1}, comprising 1.4–5.8% of total NO_3^- ($NO_3^-{}_{Total}$) loads in study watersheds during WY2016 and 2017 (Table S2).

Watershed land use percentage was a statistically significant linear predictor of nearly all $NO_3^-{}_{Atm}$ metrics. A higher percentage of agricultural land use was found to predict lower values of $\overline{\Delta^{17}O}_{Stream}$ and PE ($r^2 = 0.24$, $p < 0.0001$ for $\overline{\Delta^{17}O}_{Stream}$; $r^2 = 0.15$, $p = 0.0687$ for PE) and higher mean annual flow-weighted $NO_3^-{}_{Atm}$ concentrations ($r^2 = 0.17$, $p < 0.05$; Figure 3). These relationships were generally opposite for forested land use: after removing an outlier (GWN, our most developed watershed), higher percentages of forested land use predicted higher values of $\overline{\Delta^{17}O}_{Stream}$ ($r^2 = 22$, $p < 0.005$) and lower mean annual flow-weighted $NO_3^-{}_{Atm}$ concentrations ($r^2 = 0.30$, $p < 0.0005$) and PE ($r^2 = 0.30$, $p < 0.0005$).

Figure 2. Box and whisker plots of **a** NO_3^- concentrations, **b** $\Delta^{17}O$- NO_3^-, **c** unprocessed atmospheric NO_3^- percentages, and **d** unprocessed atmospheric NO_3^- concentrations. Watersheds are colored and grouped by general land use category: predominantly forested (> 80% forested), mixed agriculture/forest (> 25% both forested and agriculture), and predominantly developed (> 70% developed). Lines in boxes indicate median, upper and lower hinges represent 25 and 75th quartile, whiskers extend 1.5 × inter-quartile range, points beyond this range are plotted individually, and notches in boxes represent ∼ 95% confidence interval of median. Asterisk denotes single watershed with significantly different mean from all others.

Rates of terrestrial N inputs ranged from 1.3–64.9 kg N ha^{-1} y^{-1} averaged over calendar years
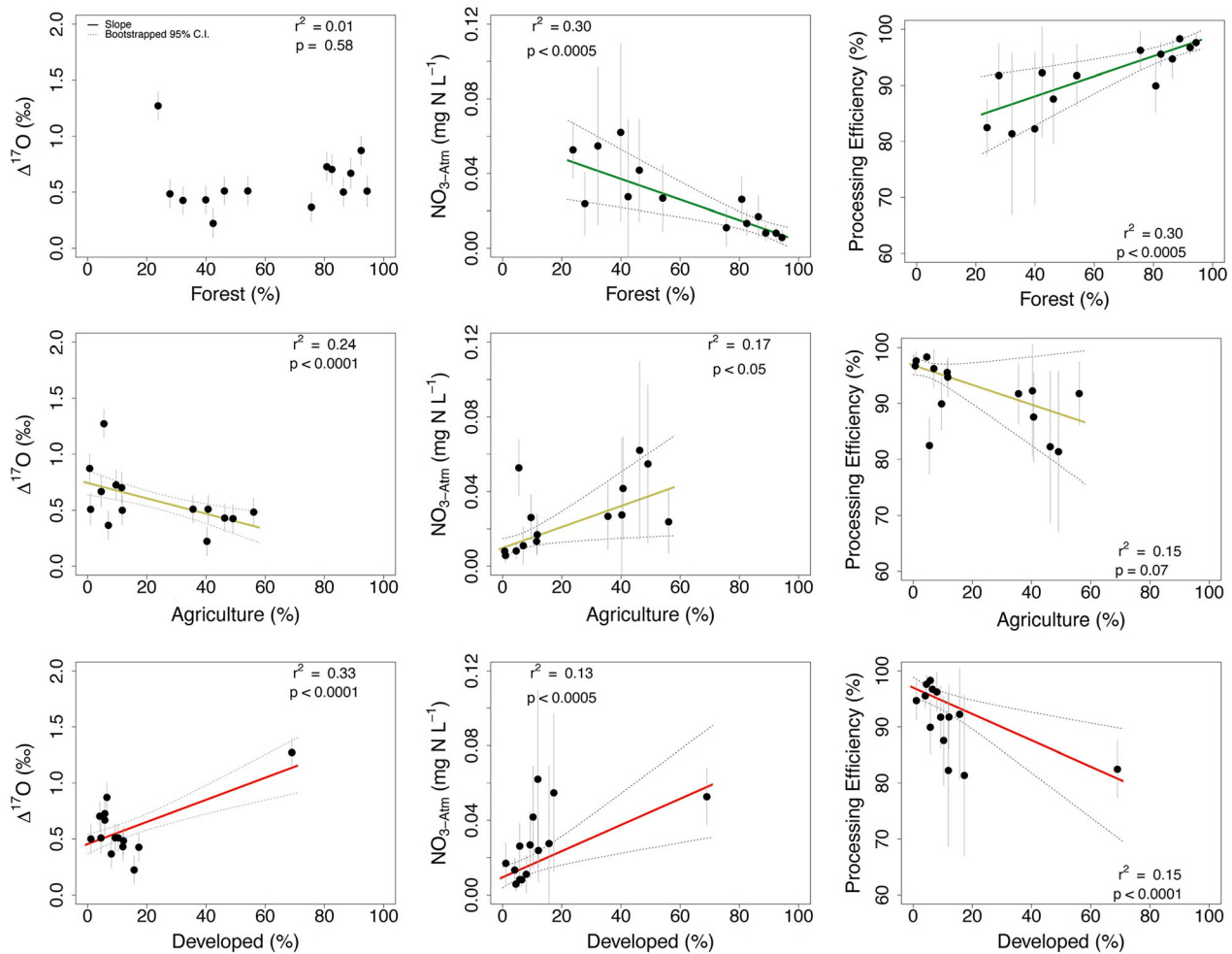
**Figure 3.** Scatter plots of land use percentages and mean annual $\Delta^{17}O$, $NO_3^-{}_{Atm}$, and processing efficiency. Solid line is weighted least squares regression line, dashed lines are bootstrapped 95% confidence intervals, r^2 is median of all bootstrapped replicates. Regressions with % developed land use should be interpreted with caution as only one watershed contained $> 20\%$ of this land use type.

2016–2017 (Table 1). Unsurprisingly, terrestrial N input rates were strongly positively correlated with agricultural ($r = 0.96$) and negatively correlated with forested land use ($r = -0.78$) and thus exhibit similar statistical relationships with $NO_3^-{}_{Atm}$ related metrics. Elevated terrestrial N input rates predicted lower $\overline{\Delta^{17}O_{Stream}}$ and PE ($r^2 = 0.25$, bootstrapped p-value < 0.0001 for $\overline{\Delta^{17}O_{Stream}}$, $r^2 = 0.20$, $p = 0.012$ for PE) and higher $NO_3^-{}_{Atm}$ ($r^2 = 0.23$, $p = 0.010$; Figure 5).

DISCUSSION

Using our results from watersheds with varied land use and our framework for interpretation (Figure 1), we present a conceptual model of proposed controls on $NO_3^-{}_{Atm}$ dynamics (Figure 4). In this

model, elevated rates of terrestrial N inputs relative to NO_3^- consumption allow proportionally more $NO_3^-{}_{Atm}$ to bypass processing and be exported in surface water. This imbalance between terrestrial N inputs and consumption additionally results in elevated $NO_3^-{}_{Total}$ concentrations, lowering the $\Delta^{17}O$ and % $NO_3^-{}_{Atm}$ of streamwater NO_3^-. Generally, watersheds with appreciable agricultural land use ($> 35\%$) are associated with elevated terrestrial N inputs (for example, from fertilizer), resulting in higher $NO_3^-{}_{Atm}$ concentrations with lower PE. Conversely, predominantly forested watersheds have lower terrestrial N inputs, with an inferred approximate balance between inputs and consumption, resulting in much of the deposited NO_3^- being processed (high PE) and thus $NO_3^-{}_{Atm}$ export being low. Impervious surfaces in developed portions of watersheds are an additional control on
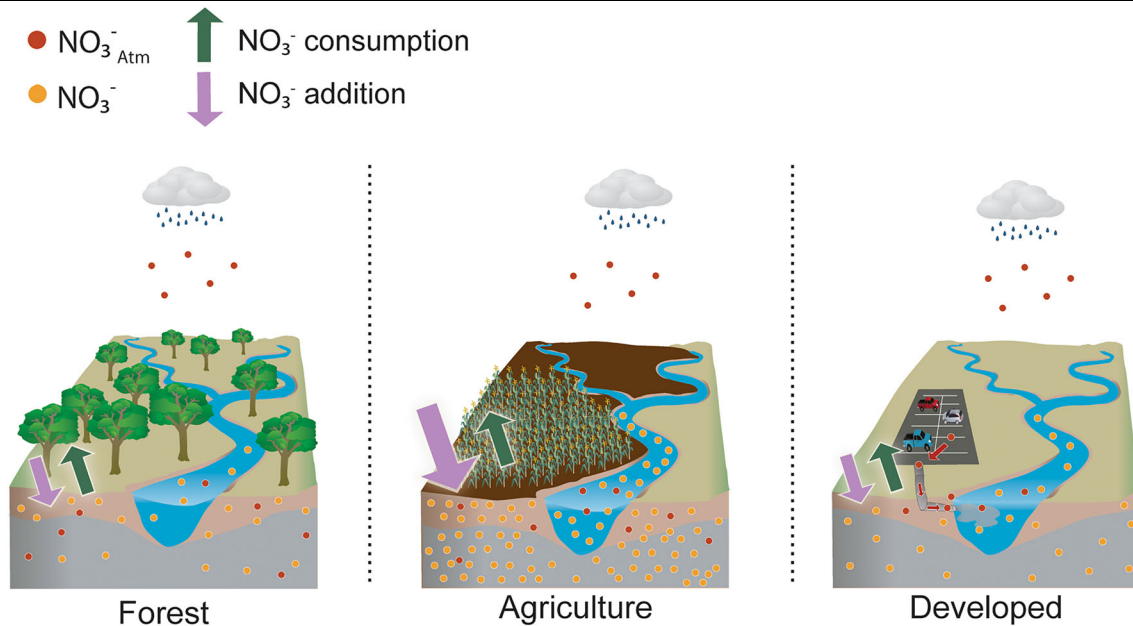
Figure 4. Conceptual model presenting the effects of land use on $NO_3^-{}_{Atm}$ (red circles) dynamics. $\Delta^{17}O$ (ratio of red to yellow circles) and $NO_3^-{}_{Atm}$ concentrations and fluxes (represented by number of red circles in streamwater) are altered between deposition and export in streamwater by rates NO_3^- addition (purple arrow) and consumption processes (green arrow), respectively. Imbalances between relative rates of NO_3^- addition and consumption (agricultural land uses), hydrologic bypassing of biotic retention mechanisms (developed land uses), and tight cycling of NO_3^- and similar rates of addition and consumption processes (forested land uses) are proposed as the land use effects on observed patterns of $NO_3^-{}_{Atm}$ dynamics (stream export and watershed processing efficiency). Symbols courtesy of the Integration and Application Network, University of Maryland Center for Environmental Science (ian.umces.edu/symbols/).

streamwater $NO_3^-{}_{Atm}$ patterns. These surfaces likely promote the rapid routing of deposited $NO_3^-{}_{Atm}$ to channels, especially during storm events, and decrease the potential for biologic processing.

Elevated rates of terrestrial N inputs to watersheds associated with land use patterns decrease $\overline{\Delta^{17}O_{Stream}}$, increase mean annual $NO_3^-{}_{Atm}$ concentrations, and decrease PE (Figure 5).

One could argue that the relationships described between land use, terrestrial N input rates, and various metrics of $NO_3^-{}_{Atm}$ dynamics result from multiplying relatively similar $\Delta^{17}O$ values by variable $NO_3^-{}_{Total}$ concentrations. However, these metrics ($\overline{\Delta^{17}O_{Stream}}$, $NO_3^-{}_{Atm}$ concentrations, and PE) account for multiple sources of uncertainty, including analytical uncertainty of $\Delta^{17}O$, β values (Eq. 1), $\Delta^{17}O$ end-members (both terrestrial and atmospheric), and annual $NO_3^-{}_{Total}$ concentrations and yields. As such, our methods represent an improvement in uncertainty quantification relative to previous research using $\Delta^{17}O$ values to quantify NO_3^- sources in streamwater (Tsunogai and others 2014; Rose and others 2015; Sabo and others 2016; Tsunogai and others 2016; Nakagawa and others

2018). The multiple sources of uncertainty in $\overline{\Delta^{17}O_{Stream}}$, $NO_3^-{}_{Atm}$ concentrations, and PE were propagated and incorporated into linear regressions with land use and terrestrial N inputs. Accounting for this uncertainty reduced r^2 values (reported as the median r^2 of 10,000 bootstraps) and increased p-values (reported as the proportion of 10,000 bootstrap slopes either greater or less than zero, depending on the specific regression) relative to simple linear regression, yet nearly all relationships between land use and terrestrial N inputs with $\overline{\Delta^{17}O_{Stream}}$, $NO_3^-{}_{Atm}$ concentrations, and PE remain significant (Figures 3 and 5). Thus, we argue that these results are a manifestation of biologic controls on $NO_3^-{}_{Atm}$ dynamics and can be interpreted as an extension of the kinetic N saturation conceptual model.

Our results suggest that biologic sinks of NO_3^- (that is, NO_3^- consumption) can be overwhelmed by high rates of N inputs, allowing proportionally more $NO_3^-{}_{Atm}$ to bypass processing and be exported in surface waters. This idea extends kinetic N saturation (Lovett and Goodale 2011) to streamwater $NO_3^-{}_{Atm}$ export and from forested to non-forested watersheds, while building on previ-
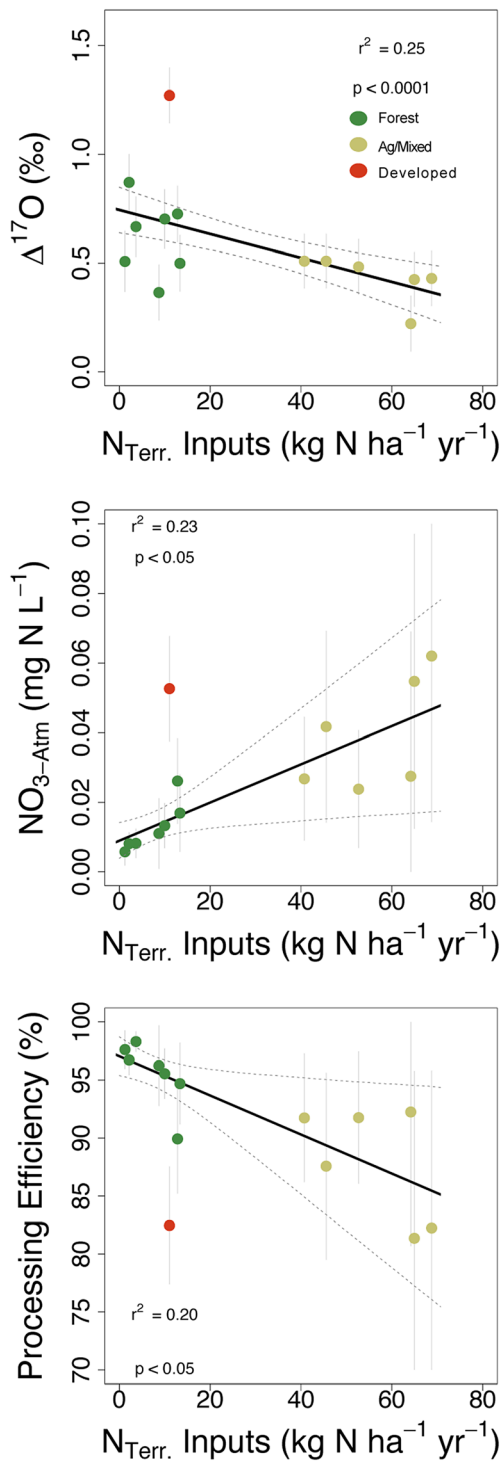
Figure 5. Scatter plots of terrestrial N input rates and mean annual $\Delta^{17}O$, $NO_3^-{}_{Atm}$, and processing efficiency. Solid line is weighted least squares regression line, dashed lines are bootstrapped 95% confidence intervals, and r^2 is median of all bootstrapped replicates. Points are colored by dominant land use.

ous work applying traditional N saturation "stages" (Ågren and Bosatta 1988; Aber and others 1989) to understanding streamwater $NO_3^-{}_{Atm}$ export (Rose and others 2015; Nakagawa and others 2018). We note, however, that our extension of the kinetic N saturation conceptual model focuses on *processing* of $NO_3^-{}_{Atm}$ while past work primarily focused on *retention* of atmospherically deposited N. We are also focusing on inputs (deposited NO_3^-) that move through watersheds to a specific sink (streamwater export) without biological transformation. Nonetheless, kinetic N saturation focuses on rates of both inputs and sinks and proposes that N saturation effects, including increased leaching of NO_3^- to surface water, are only realized when rates of inputs exceed those of sinks. Our framework for interpretation (Figure 1) can be used to infer the role of both inputs (terrestrial N inputs) and sinks (NO_3^- consumption) on $NO_3^-{}_{Atm}$ export at the watershed scale.

Large terrestrial N inputs associated with agricultural land use allow more $NO_3^-{}_{Atm}$ to be exported and reduce PE (Figures 3 and 5). An imbalance between N inputs (for example, fertilizer) and demand for NO_3^- (for example, crop uptake, denitrification) creates an accumulation of NO_3^- in soils and groundwater. NO_3^- accumulation in agricultural systems is aligned with research suggesting that N supplies in excess of demand shift soils to NO_3^- dominated "economies", as there is less competition for N and nitrifying microorganisms thrive (Schimel and Bennett 2004; Booth and others 2005). The large N inputs combined with the relative mobility of NO_3^- compared to reduced or organic N forms (Chapin and others 2011) ultimately results in increased export of NO_3^- in surface waters. The imbalance between N inputs and NO_3^- demand does not imply that NO_3^- consumption is reduced; rather, rates may even be greater in watersheds with larger terrestrial N inputs—for example, denitrification rates are generally higher in fertilized agricultural soils compared to non-fertilized soils (Barton and others 1999; Hofstra and Bouwman 2005). For a given NO_3^- consumption rate, however, a larger reservoir of NO_3^- (for example, more NO_3^- in groundwater and soil) available for consumption along hydrologic flowpaths likely allows proportionally more $NO_3^-{}_{Atm}$ to escape consumption and be exported in surface waters.

In predominantly forested watersheds with lower terrestrial N input rates, it is more likely that inputs and consumption are closer to unity on an annual basis resulting in lower $NO_3^-{}_{Atm}$ concentrations and yields, and higher PE. Reduced rates of

N inputs likely contributed to NO_3^- consumption processes imparting a seasonal signal on $NO_3^-{}_{Atm}$ concentrations, similar to previous research on streams with low $NO_3^-{}_{Total}$ concentrations (Figure S5; Barnes and Raymond 2010; Tsunogai and others 2014; Rose and others 2015; Sabo and others 2016; Hattori and others 2019). Mean $NO_3^-{}_{Atm}$ concentrations were about $1.7 \times$ higher in the dormant than growing season in watersheds with lower terrestrial N inputs rates (< 40 kg N ha^{-1} y^{-1}, $> 75\%$ forested land use; ANOVA, $p < 0.001$), whereas concentrations were not significantly different between seasons in watersheds with higher terrestrial N input rates (> 40 kg N ha^{-1} y^{-1}, $< 52\%$ forested land use; Figure S5). This result likely reflects higher rates of biologically-mediated NO_3^- consumption processes during the growing (warmer) season. For example, forest canopies can process up to 90% of $NO_3^-{}_{Atm}$ during the growing season, severely reducing the potential for $NO_3^-{}_{Atm}$ streamwater export (Inoue and others 2021). It is likely that rates of NO_3^- consumption also increase during the growing season in watersheds with elevated terrestrial N input rates, but that the amount of NO_3^- consumed is small relative to the total NO_3^- present, making it difficult to decipher the signal. One factor that may confound the interpretation of intra-annual $NO_3^-{}_{Atm}$ concentrations is the seasonal pattern of $\Delta^{17}O$ values of NO_3^- in precipitation. Seasonal patterns in $\Delta^{17}O$ values of NO_3^- in precipitation were similar across all monitoring sites in our study (Figure S3), however, suggesting that this effect would have been consistent across all watersheds.

Our results, combined with others using $\Delta^{17}O$ values of NO_3^- to quantify $NO_3^-{}_{Atm}$, supports the application and extension of kinetic N saturation to $NO_3^-{}_{Atm}$ dynamics: annual flow-weighted $NO_3^-{}_{Atm}$ concentrations are positively related to $NO_3^-{}_{Total}$ concentrations across 56 watersheds from five publications (our watersheds: $r^2 = 0.66$, $p < 0.001$; others $r^2 = 0.25$, $p < 0.001$; Figure S6). The magnitude of these relationships is slightly different between our study and others possibly due to differences in sampling frequency, which ranged from quarterly (4 per year; Tsunogai and others 2016) to weekly (Rose and others 2015), range of hydrologic conditions sampled (for example, baseflow only, baseflow and stormflow sampling), load estimation methods (Rose and others 2015; Tsunogai and others 2016; Nakagawa and others 2018) and/or watershed size (Sabo and others 2016), making it challenging to uncover potential causes of these differences in magnitude. Watersheds in these studies additionally represent diverse land uses (forested, urban, agricultural, mixed) and span NO_3^- deposition gradients (wet = 1.5–2.4 kg N ha^{-1} y^{-1}, wet + dry = 3.3–6.4 kg N ha^{-1} y^{-1}). Despite these methodological and physical differences, the direction of the relationships between $NO_3^-{}_{Atm}$ and $NO_3^-{}_{Total}$ is the same. Unfortunately, we do not have estimates of terrestrial N inputs for those watersheds included in the ancillary publications, but streamwater $NO_3^-{}_{Total}$ concentrations are a reasonable proxy of watershed-scale N inputs. $NO_3^-{}_{Total}$ concentrations integrate watershed-scale rates of both N inputs and sinks, and elevated $NO_3^-{}_{Total}$ concentrations suggest that inputs exceed sinks, allowing proportionally more $NO_3^-{}_{Atm}$ export in streamwater.

Large terrestrial N input rates result in the dilution of $\overline{\Delta^{17}O_{Stream}}$. This dilution effect is clearly evident in our results: $\overline{\Delta^{17}O_{Stream}}$ is negatively related with terrestrial N inputs ($r^2 = 0.25$, $p < 0.001$, Figure 5) and agricultural land use ($r^2 = 0.24$, $p < 0.0001$, Figure 3), even after removing an outlier with high leverage (after GWN removal: $r^2 = 0.22$, $p < 0.005$). This interpretation follows the implicit assumption that N inputs and storage are in the form of NO_3^-. We do not have data to differentiate N forms (for example, ammonium, organic N) of inputs at our study sites. Thus, we assume that the ratio of NO_3^- to total N of terrestrial N inputs and storage is similar across all watersheds. Reduction or dilution of $\Delta^{17}O$ between deposition and streamwater export assumes mixing of both $NO_3^-{}_{Atm}$ ($\Delta^{17}O \cong 25\text{‰}$) and $NO_3^-{}_{Terr}$ ($\Delta^{17}O \cong 0\text{‰}$) along hydrologic flowpaths. The negative linear relationship between terrestrial N input rates and $\overline{\Delta^{17}O_{Stream}}$ indicates mixing is likely occurring in all watersheds, with one exception: GWN, our most developed watershed.

Impervious surfaces in developed portions of watersheds can exert hydrologic controls on $\Delta^{17}O$ values, $NO_3^-{}_{Atm}$ concentrations, and PE. Overland runoff from impervious surfaces, if hydrologically connected to channels, provides a mechanism by which precipitation and dissolved substances within (for example, $NO_3^-{}_{Atm}$) can be directly routed to channels and streams (Brabec and others 2002; Tsunogai and others 2016). Direct routing of water to streams effectively short-circuits terrestrial processing that either removes $NO_3^-{}_{Atm}$ (for example, denitrification) or dilutes $\Delta^{17}O$ (for example, nitrification). This impervious area effect likely contributed to both the high $\overline{\Delta^{17}O_{Stream}}$, $NO_3^-{}_{Atm}$ concentrations and yields, and reduced PE in GWN (Table S2). Impervious surface effects

were most apparent during storm events: GWN was the only watershed in which both $\Delta^{17}O_{Stream}$ and $NO_3^-{}_{Atm}$ were significantly higher during storm events relative to baseflow (Figure S7). Our results, while derived from a single watershed, provide additional evidence supporting studies that measured elevated $NO_3^-{}_{Atm}$ using either $\delta^{18}O$ (Burns and others 2009; Hall and others 2016; Yang and Toor 2016) or $\Delta^{17}O$ (Riha and others 2014; Tsunogai and others 2016) in developed watersheds.

Measurements of $\Delta^{17}O\text{-}NO_3^-$ highlight the challenges of using $\delta^{18}O$ alone for source apportionment in mixed land use watersheds. Terrestrial N inputs associated with agricultural activities include fertilizer, some of which may be synthetic NO_3^- fertilizer. This is plausibly supported by $\delta^{18}O$ of streamwater NO_3^-; mean annual $\delta^{18}O$ was positively correlated with agricultural land use in our watersheds ($p < 0.0001$, $r^2 = 0.19$; Figure S8). Synthetic NO_3^- fertilizer is formed from tropospheric O_2 and inherits a $\delta^{18}O$ signature of $\sim 24\text{‰}$ (Michalski and others 2015). Alternatively, the relationship between mean annual $\delta^{18}O$ and agricultural land use could be interpreted as the result of increased denitrification in agricultural areas, which can increase the $\delta^{18}O$ of residual NO_3^- (Böttcher and others 1990; Kendall and others 2007). These competing interpretations demonstrate one of the difficulties in using $\delta^{18}O$ alone to quantify streamwater $NO_3^-{}_{Atm}$ in mixed land use watersheds; it is impossible to assign a specific $\delta^{18}O$ $NO_3^-{}_{Terr}$ end-member to watersheds with multiple sources of $NO_3^-{}_{Terr.}$ The use of $\Delta^{17}O$ as a tracer is also limited in watersheds with large inputs of terrestrial N that result in elevated $NO_3^-{}_{Total}$ streamwater export relative to $NO_3^-{}_{Atm}$ deposition. For example, in a hypothetical watershed with 10 kg N ha^{-1} y^{-1} $NO_3^-{}_{Total}$ streamwater export, 1 kg N ha^{-1} y^{-1} of $NO_3^-{}_{Atm}$ deposition and a PE = 80%, $\overline{\Delta^{17}O_{Stream}}$ would only equal 0.5‰. As the ratio of $NO_3^-{}_{Atm}$ deposition to $NO_3^-{}_{Total}$ streamwater export decreases, $\overline{\Delta^{17}O_{Stream}}$ also decreases for a constant PE, making it increasingly difficult to detect $NO_3^-{}_{Atm}$ in streamwater regardless of the isotopic tracer (Figure S9).

In conclusion, land use influenced all metrics of $NO_3^-{}_{Atm}$ dynamics ($\overline{\Delta^{17}O_{Stream}}$, $NO_3^-{}_{Atm}$ concentrations and yields, PE). Insights into watershed-scale, land -use specific processes affecting $NO_3^-{}_{Atm}$ were possible through measurements of $\Delta^{17}O$, a conservative tracer of $NO_3^-{}_{Atm}$, on streamwater samples collected under a range of hydrologic conditions across numerous watersheds. Agricul-

tural land use with elevated rates of terrestrial N inputs was associated with increased streamwater export of $NO_3^-{}_{Atm}$ relative to predominantly forested watersheds. Large terrestrial N inputs in agricultural lands overwhelmed N sinks and allowed proportionally more $NO_3^-{}_{Atm}$ to escape consumption (denitrification, assimilation, immobilization) and be exported in surface waters. Development in watersheds likely increased $NO_3^-{}_{Atm}$ export due to hydrologic connectivity of overland flowpaths that bypass potential biological processing, supporting previous $NO_3^-{}_{Atm}$ research in developed watersheds. Accordingly, future changes to land use patterns and rates of terrestrial N inputs to watersheds will likely increase (that is, urbanization, increased fertilizer application rates) or decrease (that is, reforestation of agricultural lands, reduced fertilizer application rates) the fraction of deposited $NO_3^-{}_{Atm}$ that is exported in streamwater that directly contributes to nutrient pollution of downstream ecosystems.

DATA AVAILABILITY

Data are available at https://github.com/jbost1458/Bostic_etal_Ecosystems2021.

REFERENCES

Aber JD, Nadelhoffer KJ, Steudler P, Melillo JM. 1989. Nitrogen Saturation in Northern Forest Ecosystems: Excess nitrogen from fossil fuel combustion may stress the biosphere. BioScience 39:378–386.

Ågren GI, Bosatta E. 1988. Nitrogen saturation of terrestrial ecosystems. Environmental Pollution 54:185–197.

Barnes RT, Raymond PA. 2010. Land-use controls on sources and processing of nitrate in small watersheds: insights from dual isotopic analysis. Ecological Applications 20:1961–1978.

Barnes RT, Raymond PA, Casciotti KL. 2008. Dual isotope analyses indicate efficient processing of atmospheric nitrate by forested watersheds in the northeastern U.S. Biogeochemistry 90:15–27.

Barton L, McLay CDA, Schipper LA, Smith CT. 1999. Annual denitrification rates in agricultural and forest soils: a review. Soil Research 37:1073–1094.

Bevington PR, Robinson DK. 2003. Data reduction and error analysis for the physical sciences. New York: McGraw-Hill. p 338p.

Böhlke JK, Hatzinger PB, Sturchio NC, Gu B, Abbene I, Mroczkowski SJ. 2009. Atacama perchlorate as an agricultural contaminant in groundwater: Isotopic and chronologic evidence from Long Island, New York. Environmental Science & Technology 43:5619–5625.

Böhlke JK, Mroczkowski SJ, Coplen TB. 2003. Oxygen isotopes in nitrate: new reference materials for ^{18}O:^{17}O:^{16}O measurements and observations on nitrate-water equilibration. Rapid Communications in Mass Spectrometry 17:1835–1846.

Booth MS, Stark JM, Rastetter E. 2005. Controls on nitrogen cycling in terrestrial ecosystems: A synthetic analysis of literature data. Ecological Monographs 75:139–157.

Böttcher J, Strebel O, Voerkelius S, Schmidt HL. 1990. Using isotope fractionation of nitrate-nitrogen and nitrate-oxygen for evaluation of microbial denitrification in a sandy aquifer. Journal of Hydrology 114:413–424.

Bourgeois I, Savarino J, Caillon N, Angot H, Barbero A, Delbart F, Voisin D, Clément J-C. 2018a. Tracing the fate of atmospheric nitrate in a subalpine watershed using $\Delta^{17}O$. Environmental Science & Technology 52:5561–5570.

Bourgeois I, Savarino J, Némery J, Caillon N, Albertin S, Delbart F, Voisin D, Clément J-C. 2018b. Atmospheric nitrate export in streams along a montane to urban gradient. Science of the Total Environment 633:329–340.

Boyer EW, Goodale CL, Jaworski NA, Howarth RW. 2002. Anthropogenic nitrogen sources and relationships to riverine nitrogen export in the northeastern U.S.A. Biogeochemistry 57:137–169.

Brabec E, Schulte S, Richards PL. 2002. Impervious surfaces and water quality: A review of current literature and its implications for watershed planning. Journal of Planning Literature 16:499–514.

Burns DA, Boyer EW, Elliott EM, Kendall C. 2009. Sources and transformations of nitrate from streams draining varying land uses: evidence from dual isotope analysis. Journal of Environmental Quality 38:1149–1159.

Burns DA, Kendall C. 2002. Analysis of $\delta^{15}N$ and $\delta^{18}O$ to differentiate NO_3^- sources in runoff at two watersheds in the Catskill Mountains of New York. Water Resources Research 38:9.1-9.11.

Casciotti KL, Sigman DM, Hastings MG, Böhlke J, Hilkert A. 2002. Measurement of the oxygen isotopic composition of nitrate in seawater and freshwater using the denitrifier method. Analytical Chemistry 74:4905–4912.

Chapin FS, Matson PA, Vitousek P. 2011. Principles of Terrestrial Ecosystem Ecology. New York: Springer Science & Business Media. p 529p.

Cheseapeake Bay Program, 2020. Cheseapeake Assessment and Scenario Tool (CAST) Version 2019. Chesapeake Bay Program Office, Last accessed June, 2021.

Clark CM, Tilman D. 2008. Loss of plant species after chronic low-level nitrogen deposition to prairie grasslands. Nature 451:712–715.

Driscoll CT, Lawrence GB, Bulger AJ, Butler TJ, Cronan CS, Eagar C, Lambert KF, Likens GE, Stoddard JL, Weathers KC. 2001. Acidic deposition in the northeastern United States: Sources and inputs. BioScience 51:180–198.

Eshleman KN, Sabo RD. 2016. Declining nitrate-N yields in the Upper Potomac River Basin: What is really driving progress under the Chesapeake Bay restoration? Atmospheric Environment 146:280–289.

Eshleman KN, Sabo RD, Kline KM. 2013. Surface water quality is improving due to declining atmospheric N deposition. Environmental Science & Technology 47:12193–12200.

Fang Y, Koba K, Makabe A, Takahashi C, Zhu W, Hayashi T, Hokari AA, Urakawa R, Bai E, Houlton BZ, Xi D, Zhang S, Matsushita K, Tu Y, Liu D, Zhu F, Wang Z, Zhou G, Chen D, Makita T, Toda H, Liu X, Chen Q, Zhang D, Li Y, Yoh M. 2015. Microbial denitrification dominates nitrate losses from forest ecosystems. Proceedings of the National Academies of Sciences of the United States of America 112:1470–1474.

Galloway JN, Aber JD, Erisman JW, Seitzinger SP, Howarth RW, Cowling EB, Cosby BJ. 2003. The nitrogen cascade. BioScience 53:341–356.

Galloway JN, Dentener FJ, Capone DG, Boyer EW, Howarth RW, Seitzinger SP, Asner GP, Cleveland CC, Green PA, Holland EA, Karl DM, Michaels AF, Porter JH, Townsend AR, Vöosmarty CJ. 2004. Nitrogen cycles: past, present, and future. Biogeochemistry 70:153–226.

Grigal DF. 2012. Atmospheric deposition and inorganic nitrogen flux. Water, Air, & Soil Pollution 223:3565–3575.

Groffman PM, Law NL, Belt KT, Band LE, Fisher GT. 2004. Nitrogen fluxes and retention in urban watershed ecosystems. Ecosystems 7:393–403.

Hall SJ, Weintraub SR, Eiriksson D, Brooks PD, Baker MA, Bowen GJ, Bowling DR. 2016. Stream nitrogen inputs reflect groundwater across a snowmelt-dominated montane to urban watershed. Environmental Science & Technology 50:1137–1146.

Hattori S, Nuñez Palma Y, Itoh Y, Kawasaki M, Fujihara Y, Takase K, Yoshida N. 2019. Isotopic evidence for seasonality of microbial internal nitrogen cycles in a temperate forested catchment with heavy snowfall. Science of the Total Environment 690:290–299.

Hofstra N, Bouwman AF. 2005. Denitrification in agricultural soils: summarizing published data and estimating global annual rates. Nutrient Cycling in Agroecosystems 72:267–278.

Homer C, Dewitz J, Jin S, Xian G, Costello C, Danielson P, Gass L, Funk M, Wickham J, Stehman S, Auch R, Riitters K. 2020. Conterminous United States land cover change patterns 2001–2016 from the 2016 National Land Cover Database. ISPRS Journal of Photogrammetry and Remote Sensing 162:184–199.

Howarth R, Anderson D, Cloern J, Elfring C, Hopkinson C, Lapointe B, Malone T, Marcus N, McGlathery K, Sharpley AN, Walker D. 2000. Nutrient pollution of coastal rivers, bays, and seas. Issues in Ecology 7:1–15.

Inoue T, Nakagawa F, Shibata H, Tsunogai U. 2021. Vertical Changes in the Flux of Atmospheric Nitrate From a Forest Canopy to the Surface Soil Based on Δ17O Values. Journal of Geophysical Research: Biogeosciences 126: e2020JG005876.

Jordan TE, Correll DL, Weller DE. 1997. Relating nutrient discharges from watersheds to land use and streamflow variability. Water Resources Research 33:2579–2590.

Kaiser J, Hastings MG, Houlton BZ, Röckmann T, Sigman DM. 2007. Triple oxygen isotope analysis of nitrate using the denitrifier method and thermal decomposition of N_2O. Analytical Chemistry 79:599–607.

Kaushal SS, Groffman PM, Band LE, Elliott EM, Shields CA, Kendall C. 2011. Tracking nonpoint source nitrogen pollution in human-impacted watersheds. Environmental Science & Technology 45:8225–8232.

Kaushal SS, Groffman PM, Band LE, Shields CA, Morgan RP, Palmer MA, Belt KT, Swan CM, Findlay SE, Fisher GT. 2008. Interaction between urbanization and climate variability amplifies watershed nitrate export in Maryland. Environmental Science & Technology 42:5872–5878.

Kemp WM, Boynton WR, Adolf JE, Boesch DF, Boicourt WC, Brush G, Cornwell JC, Fisher TR, Glibert PM, Hagy JD. 2005. Eutrophication of Chesapeake Bay: historical trends and ecological interactions. Marine Ecology Progress Series 303:1–29.

Kendall C, Campbell DH, Burns DA, Shanley JB, Silva SR, Chang CC. 1995. Tracing sources of nitrate in snowmelt runoff using the oxygen and nitrogen isotopic compositions of nitrate. IAHS Publications-Series of Proceedings and Reports-Intern Assoc Hydrological Sciences 228:339–348.

Kendall C, Elliott EM, Wankel SD. 2007. Tracing anthropogenic inputs of nitrogen to ecosystems. In: RH Michener and K. Lajtha (Eds.), Stable Isotopes in Ecology and Environmental Science 2nd edition, Blackwell Publishing: 375–449.

Li Y, Schichtel BA, Walker JT, Schwede DB, Chen X, Lehmann CM, Puchalski MA, Gay DA, Collett JL. 2016. Increasing importance of deposition of reduced nitrogen in the United States. Proceedings of the National Academy of Sciences 113:5874–5879.

Lovett GM, Goodale CL. 2011. A new conceptual model of nitrogen saturation based on experimental nitrogen addition to an oak forest. Ecosystems 14:615–631.

Lovett GM, Lindberg SE. 1993. Atmospheric deposition and canopy interactions of nitrogen in forests. Canadian Journal of Forest Research 23:1603–1616.

McDonald JH. 2009. Handbook of biological statistics: Sparky House Publishing Baltimore, MD.

Michalski G, Bhattacharya S, Mase DF. 2012. Oxygen isotope dynamics of atmospheric nitrate and its precursor molecules. In: M. Baskaran (ed.), Handbook of Environmental Isotope Geochemistry, Springer: 613–635.

Michalski G, Kolanowski M, Riha KM. 2015. Oxygen and nitrogen isotopic composition of nitrate in commercial fertilizers, nitric acid, and reagent salts. Isotopes in Environmental and Health Studies 51:382–391.

Michalski G, Meixner T, Fenn M, Hernandez L, Sirulnik A, Allen E, Thiemens M. 2004. Tracing atmospheric nitrate deposition in a complex semiarid ecosystem using Δ17O. Environmental Science & Technology 38:2175–2181.

Michalski G, Savarino J, Böhlke JK, Thiemens M. 2002. Determination of the total oxygen isotopic composition of nitrate and the calibration of a Δ17O nitrate reference material. Analytical Chemistry 74:4989–4993.

Michalski G, Scott Z, Kabiling M, Thiemens MH. 2003. First measurements and modeling of Δ17O in atmospheric nitrate. Geophysical Research Letters 30.

Nakagawa F, Tsunogai U, Obata Y, Ando K, Yamashita N, Saito T, Uchiyama S, Morohashi M, Sase H. 2018. Export flux of unprocessed atmospheric nitrate from temperate forested catchments: a possible new index for nitrogen saturation. Biogeosciences 15:7025–7042.

Nelson DM, Tsunogai U, Ding D, Ohyama T, Komatsu DD, Nakagawa F, Noguchi I, Yamaguchi T. 2018. Triple oxygen isotopes indicate urbanization affects sources of nitrate in wet and dry atmospheric deposition. Atmospheric Chemistry and Physics 18:6381–6392.

National Atmospheric Deposition Program (NRSP-3). 2021. NADP Program Office, Wisconsin State Laboratory of Hygiene, 465 Henry Mall, Madison, WI 53706.

Osaka K, Kugo T, Komaki N, Nakamura T, Nishida K, Nagafuchi O. 2016. Atmospheric nitrate leached from small forested watersheds during rainfall events: Processes and quantitative evaluation. Journal of Geophysical Research: Biogeosciences 121:2030–2048.

R Development Core Team. 2019. R: A language and environment for statistical computing. Vienna, Austria: R Foundation for Statistical Computing.

Riha KM, Michalski G, Gallo EL, Lohse KA, Brooks PD, Meixner T. 2014. High atmospheric nitrate inputs and nitrogen turnover in semi-arid urban catchments. Ecosystems 17:1309–1325.

Rose LA, Elliott EM, Adams MB. 2015. Triple nitrate isotopes indicate differing nitrate source contributions to streams across a nitrogen saturation gradient. Ecosystems 18:1209–1223.

Sabo RD, Nelson DM, Eshleman KN. 2016. Episodic, seasonal, and annual export of atmospheric and microbial nitrate from a temperate forest. Geophysical Research Letters 43:683–691.

Schimel, JP, Bennett, J. Nitrogen mineralization: Challenges of a changing paradigm. Ecology 85: 591–602.

Sebestyen SD, Ross DS, Shanley JB, Elliott EM, Kendall C, Campbell JL, Dail DB, Fernandez IJ, Goodale CL, Lawrence GB, Lovett GM, McHale PJ, Mitchell MJ, Nelson SJ, Shattuck MD, Wickman TR, Barnes RT, Bostic JT, Buda AR, Burns DA, Eshleman KN, Finlay JC, Nelson DM, Ohte N, Pardo LH, Rose LA, Sabo RD, Schiff SL, Spoelstra J, Williard KWJ. 2019. Unprocessed atmospheric nitrate in waters of the northern forest region in the U.S. and Canada. Environmental Science & Technology 53:3620–3633.

Sigman DM, Casciotti KL, Andreani M, Barford C, Galanter M, Böhlke J. 2001. A bacterial method for the nitrogen isotopic analysis of nitrate in seawater and freshwater. Analytical Chemistry 73:4145–4153.

Sprague LA. 2001. Effects of storm-sampling frequency on estimation of water-quality loads and trends in two tributaries to Chesapeake Bay in Virginia. US Geological Survey Water-Resources Investigations Report 01-4136.

Sudduth EB, Perakis SS, Bernhardt ES. 2013. Nitrate in watersheds: Straight from soils to streams? Journal of Geophysical Research: Biogeosciences 118:291–302.

Tørseth K, Aas W, Breivik K, Fjæraa AM, Fiebig M, Hjellbrekke AG, Lund Myhre C, Solberg S, Yttri KE. 2012. Introduction to the European Monitoring and Evaluation Programme (EMEP) and observed atmospheric composition change during 1972–2009. Atmospheric Chemistry and Physics 12:5447–5481.

Tsunogai U, Komatsu DD, Daita S, Kazemi GA, Nakagawa F, Noguchi I, Zhang J. 2010. Tracing the fate of atmospheric nitrate deposited onto a forest ecosystem in Eastern Asia using $\Delta^{17}O$. Atmos. Chem. Phys. 10:1809–1820.

Tsunogai U, Komatsu DD, Ohyama T, Suzuki A, Nakagawa F, Noguchi I, Takagi K, Nomura M, Fukuzawa K, Shibata H. 2014. Quantifying the effects of clear-cutting and strip-cutting on nitrate dynamics in a forested watershed using triple oxygen isotopes as tracers. Biogeosciences 11:5411–5424.

Tsunogai U, Miyauchi T, Ohyama T, Komatsu DD, Nakagawa F, Obata Y, Sato K, Ohizumi T. 2016. Accurate and precise quantification of atmospheric nitrate in streams draining land of various uses by using triple oxygen isotopes as tracers. Biogeosciences 13:3441–3459.

United States Geological Survey. 2016. The StreamStats program, online at http://streamstats.usgs.gov.

PRISM Climate Group, Oregon State University, http://prism.oregonstate.edu, created 4 Feb 2004.

Yang Y-Y, Toor GS. 2016. $\delta^{15}N$ and $\delta^{18}O$ reveal the sources of nitrate-nitrogen in urban residential stormwater runoff. Environmental Science & Technology 50:2881–2889.

Young ED, Galy A, Nagahara H. 2002. Kinetic and equilibrium mass-dependent isotope fractionation laws in nature and their geochemical and cosmochemical significance. Geochimica Et Cosmochimica Acta 66:1095–1104.

Yu Z, Elliott EM. 2018. Probing soil nitrification and nitrate consumption using $\Delta^{17}O$ of soil nitrate. Soil Biology and Biochemistry 127:187–199.

Zhang Q, Hirsch RM. 2019. River water-quality concentration and flux estimation can be improved by accounting for serial correlation through an autoregressive model. Water Resources Research 55:9705–9723.